Supplement of Atmos. Meas. Tech., 18, 7231–7242, 2025
https://doi.org/10.5194/amt-18-7231-2025-supplement

Atmospheric Measurement Techniques
Open Access
EGU

Supplement of

Development and use of a lightweight sampling system for height-selective UAV-based measurements of organic aerosol particles

Christine Borchers et al.

Correspondence to: Thorsten Hoffmann (t.hoffmann@uni-mainz.de)

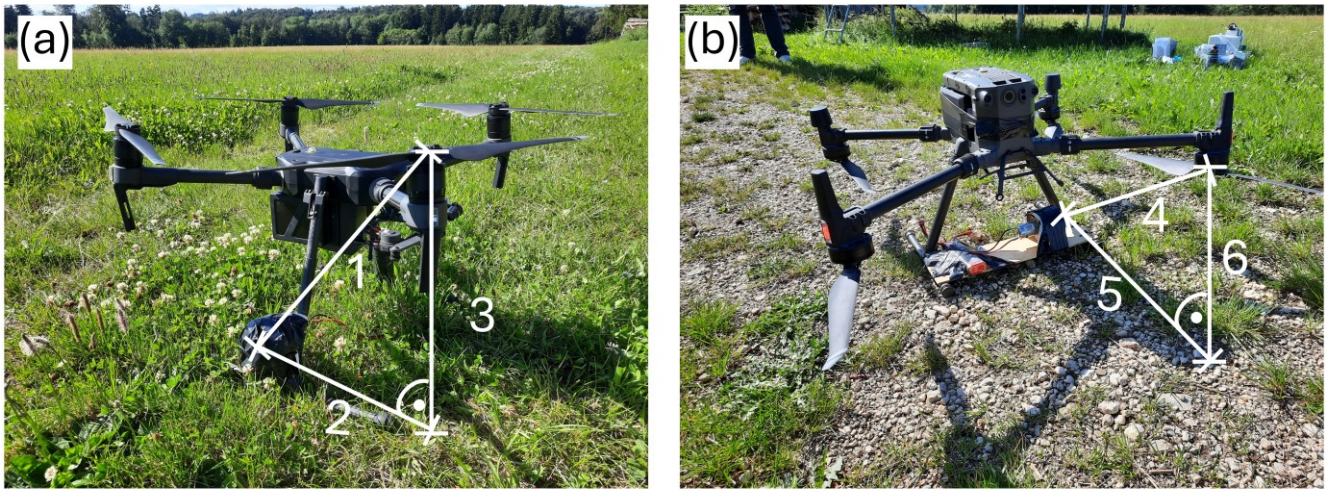

Figure S1: Photo of the filter holder attached to the landing gear at the UAV dji m200 (a) and at plate between the landing gear of the dji m300 (b). The white lines indicate measured distances. Line 1 (51 cm) is the diagonal distance between the collector and the rotor of the UAV. Line 2 (26 cm) is the distance between the collector and the perpendicular to the rotor of the UAV, and line 3 (44 cm) is the height difference between the collector and the rotor for the UAV(dji m200). Line 4 (36 cm) is the diagonal distance between the collector and the rotor of the UAV. Line 5 (30 cm) is the distance between the collector and the perpendicular to the rotor of the UAV, and line 6 (19 cm) is the height difference between the collector and the rotor for the UAV(dji m300).

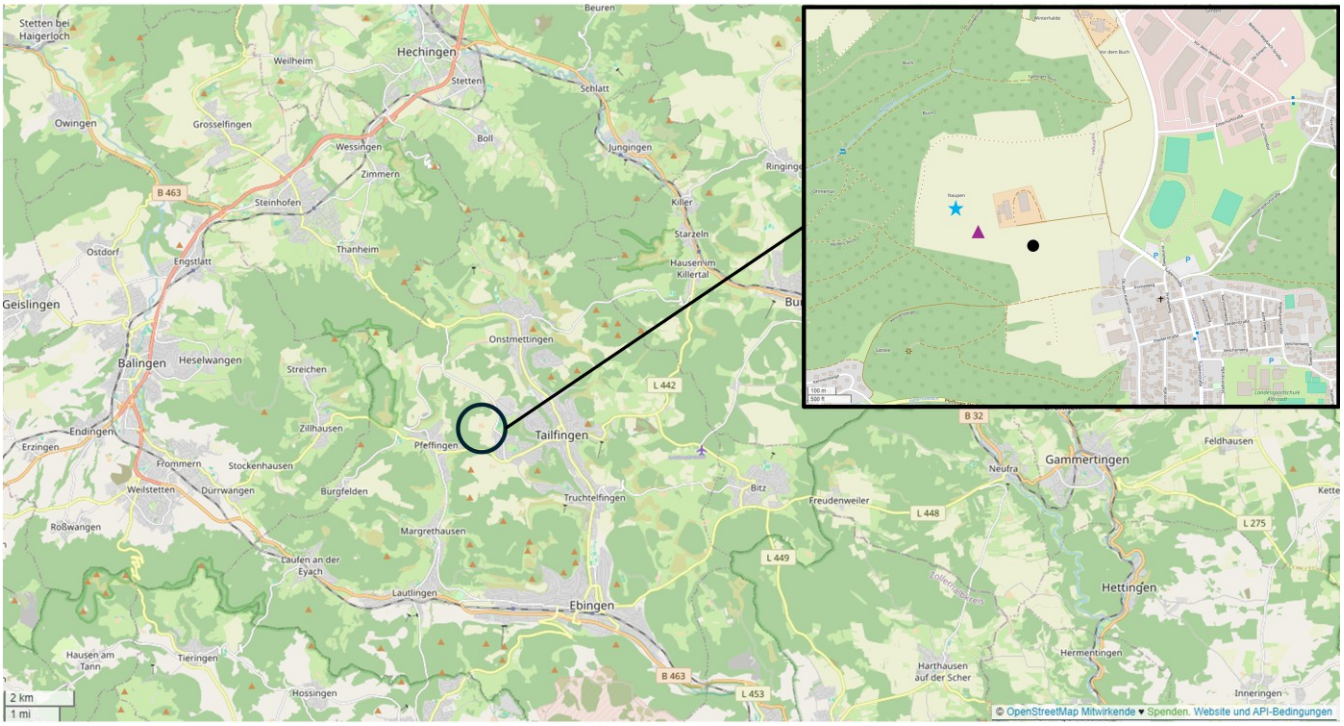

20 **Figure S2: Map (© OpenStreetMap contributors 2025. Distributed under the Open Data Commons Open Database License (ODbL) v1.0.) showing the measurement site (close to Albstadt, southern Germany), which is surrounded in all directions by a mixture of forest, agricultural land, and urban infrastructure. The black circle represents the measurement site, which is shown in greater detail within the black box. The symbols indicate the approximate locations for the UAV measurements: a blue star (djim300), a purple triangle (dji m200), and a black dot (FLab).**

25

S1 Determination of the concentration

The extraction solution was not concentrated to dryness to prevent loss of semi-volatile compounds, so the volume prior to HPLC-MS analysis is unknown. To overcome this issue, a known amount of camphor sulfonic acid was added to both the calibration solutions and the samples as internal standard. This ensured that the concentration of all solutions would correspond to 35 ng/mL of the internal standard if the samples had the targeted 50 µL volume. In order to perform the volume correction, the mean value of the signal area of the camphor sulfonic acid of all calibration solutions is calculated. Following this, the ratio of the signal area for the respective sample to this mean value is multiplied by the concentration of the analytes determined by the calibration. This allows the concentration of the analytes to be obtained as if they were dissolved in 50 µL.

As the HPLC-MS analysis only determines the concentration of the sample in the extraction solution it is necessary to determine the concentration in the aerosol (c(compound). This is achieved by first calculating the mass m(compound) on the filter according to the following equation S1, with V_{solution} representing the Volume and c_{solution}(compound) symbolizing the blank-corrected concentration of the compound in the extraction solution prior to the HPLC-MS measurement.

$$m(\text{compound}) = c_{\text{solution}}(\text{compound}) \cdot V_{\text{solution}} \quad \text{(S1)}$$

The collected air volume (V_{air}) is then determined by integrating the linear equation of the fit for the flow (Q) (Equation S2) through the filter holder, which leads to Equation S3. In the following equations t is the sampling time.

$$Q = (-0.41 \pm 0.01)\, S\text{LPM min}^{-1} \cdot t + (102.8 \pm 0.2)\ \text{SLPM} \quad \text{(S2)}$$

$$V_{\text{air}} = \frac{(-0.027 \pm 0.002)}{2}\ \text{SLPM min}^{-1} \cdot t^2 + (18.97 \pm 0.04)\text{SLPM} \cdot t \quad \text{(S3)}$$

Since the flow through the collector is pressure dependent, it must be corrected for the different pressures at different heights (1.5 m: 920 hPa; 120 m: 907 mbar; 500 m: 870 mbar; measured by FLab). The linear fit for the dependence of flow on pressure (*Q(p)*) is used for the correction (Equation S4).

$$Q(P) = (0.20 \pm 0.01)\ \text{SLPM hPa}^{-1} \cdot p + (-93 \pm 12) \quad \text{(S4)}$$

The collected air volume$V_{\text{air}}(p)$ is subsequently corrected according to Equation S5. The flow at 980 hPa is utilized as a reference because the time dependence was determined at this air pressure.

$$V_{\text{air}}(p) = V_{\text{air}} \cdot \frac{Q(p)}{Q(980\ \text{hPa})} \quad \text{(S5)}$$

The concentration of the compound of interest can then be calculated as shown in Equation S6.

$$c(\text{compound}) = \frac{m(\text{compound})}{V_{\text{air}}(p)} \quad \text{(S6)}$$

S2 Chemicals

Table S1: Chemical compounds used in this study, including their respective purities.

Compound	Label	purity
cis-pinic acid	Synthesized	N/A
terpenylic acid	Synthesized	N/A
terebic acid	Sigma Aldrich	N/A
salicylic acid	Sigma Aldrich	99%
4-hydroxybenzaldehyde	Sigma Aldrich	>97.5%
4-nitrophenol	Alfa Aesar	99%
2,6-dimethyl-4-nitrophenol	Merck KGaA	N/A
2,4-dinitrophenol	Sigma Aldrich	>98%

Table S2: Measured concentration of pinic acid, 4-nitrophenol, terebic acid and 2,6-dimethyl-4-nitrophenol, of the three measurement setups (no UAV; dji m300; dji m200) during three measurement flights.

Flight	UAV	Pinic acid		Terebic acid		4-Nitrophenol		2,6-Dimethyl-4-nitrophenol	
		Concentration / ng m^{-3}	Error	Concentration / ng m^{-3}	Error	Concentration / ng m^{-3}	Error	Concentration / ng m^{-3}	Error
1	-	1.91	0.05	0.53	0.03	1.67	0.06	0.20	0.004
	Dji m300	1.42	0.06	0.39	0.02	1.20	0.03	0.17	0.004
	Dji m200	1.61	0.07	0.44	0.02	1.46	0.03	0.17	0.00
2	-	1.71	0.05	0.55	0.03	1.43	0.05	0.23	0.01
	Dji m300	1.71	0.07	0.52	0.03	1.42	0.04	0.24	0.005
	Dji m200	1.72	0.08	0.54	0.02	1.52	0.08	0.25	0.01
3	-	1.87	0.09	0.50	0.03	2.63	0.10	0.68	0.02
	Dji m300	1.97	0.08	0.58	0.02	2.73	0.06	0.69	0.01
	Dji m200	2.09	0.06	0.57	0.02	2.90	0.06	0.78	0.02

Table S3: Measured concentration of the biogenic marker compounds pinic acid, terpenylic acid and terebic acid at the different heights and times (all times are in UTC+2).

Time	Height / m	Pinic acid		Terpenylic acid		Terebic acid	
		Concentration / ng m^{-3}	Error	Concentration / ng m^{-3}	Error	Concentration / ng m^{-3}	Error
10:35 am	1.5	1.92	0.51	0.66	0.18	1.11	0.30
	120	2.22	0.60	0.84	0.23	1.40	0.38
	500	1.40	0.39	0.56	0.16	0.81	0.23
1:35 pm	1.5	3.01	0.80	1.17	0.31	2.07	0.55
	120	3.46	0.93	1.20	0.33	2.02	0.54
	500	2.62	0.73	0.91	0.26	1.58	0.44
4:30 pm	1.5	2.80	0.75	1.14	0.31	2.29	0.61
	120	4.14	1.11	1.81	0.49	3.13	0.84
	500	3.35	0.94	1.40	0.39	2.37	0.66

Table S4: Measured concentration of the biomass burning and anthropogenic marker compounds salicylic acid, 4-hydroxybenzaledhyde. 4-nitrophenol, 2,4-dinitrophenol at different heights and times (all times are in UTC+2).

Time	Height / m	Salicylic acid		4-Hydroxy-benzaldehyde		4-Nitrophenol		2,6-Dimethyl-4-nitrophenol		2,4-Dinitrophenol	
		Concentration / ng m^{-3}	Error	Concentration / ng m^{-3}	Error	Concentration / ng m^{-3}	Error	Concentration / ng m^{-3}	Error	Concentration / ng m^{-3}	Error
10:35 am	1.5	0.09	0.08	0.11	0.06	1.03	0.28	0.03	0.04	0.20	0.09
	120	0.45	0.16	0.28	0.10	1.40	0.39	0.04	0.04	0.30	0.12
	500	0.01	0.06	0.08	0.05	0.82	0.24	0.02	0.03	0.12	0.07
1:35 pm	1.5	0.11	0.08	0.19	0.07	0.41	0.13	0.02	0.03	0.07	0.07
	120	0.00	0.09	0.18	0.08	0.48	0.16	0.02	0.04	0.13	0.09
	500	0.16	0.08	0.24	0.08	0.39	0.12	0.02	0.03	0.06	0.06
4:30 pm	1.5	0.05	0.07	0.20	0.07	0.20	0.09	0.01	0.03	0.04	0.07
	120	0.16	0.10	0.39	0.12	0.41	0.14	0.02	0.04	0.07	0.08
	500	0.21	0.09	0.24	0.08	0.30	0.11	0.01	0.03	0.05	0.06

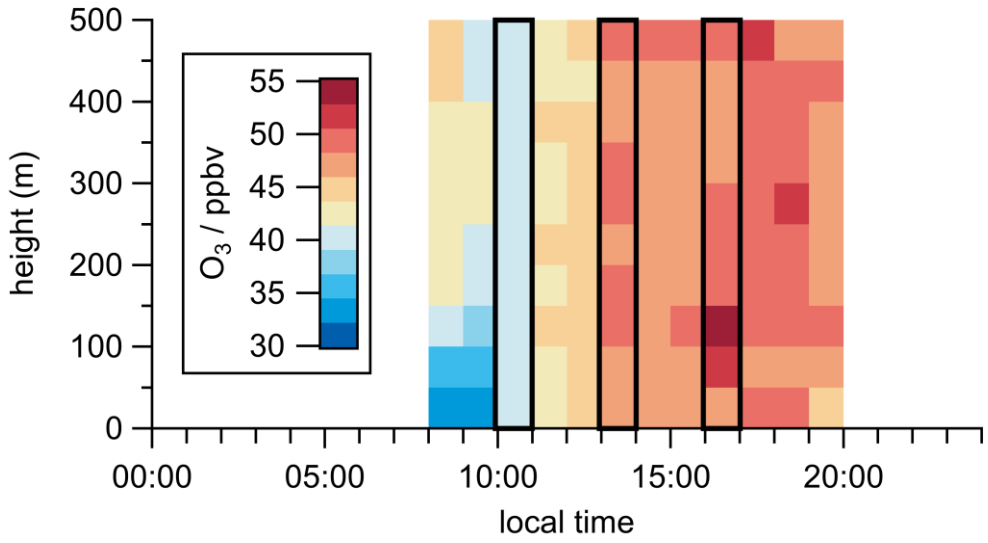

Figure S3: Measured ozone concentration versus time of day. The measurements were carried out hourly in an altitude range from 0 to 500 m above ground level (AGL). The black boxes indicate the time intervals during when the parallel UAV flights were conducted.

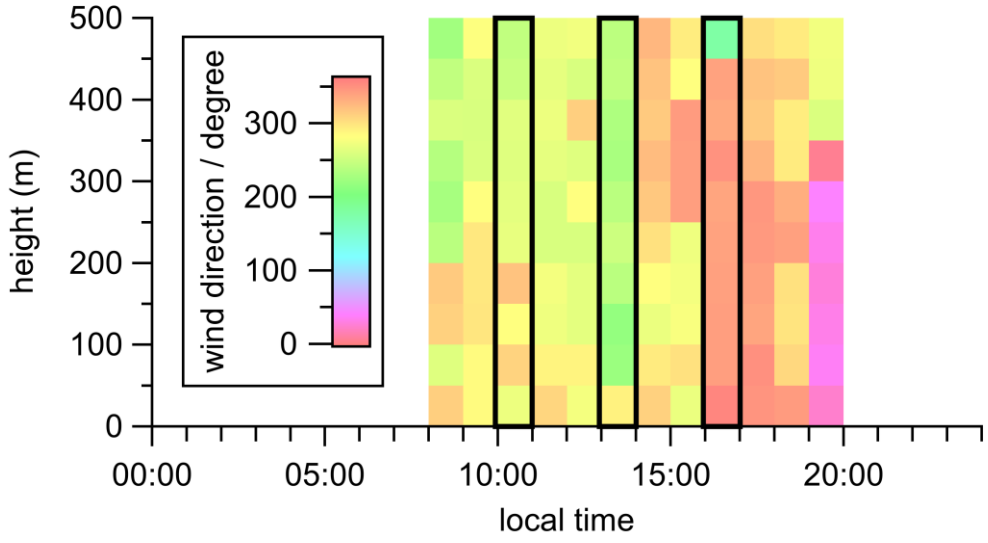

Figure S4: Measured wind direction versus time of day. The measurements were carried out hourly in an altitude range from 0 to 500 m. The black boxes indicate the time intervals during when the parallel UAV flights were conducted.

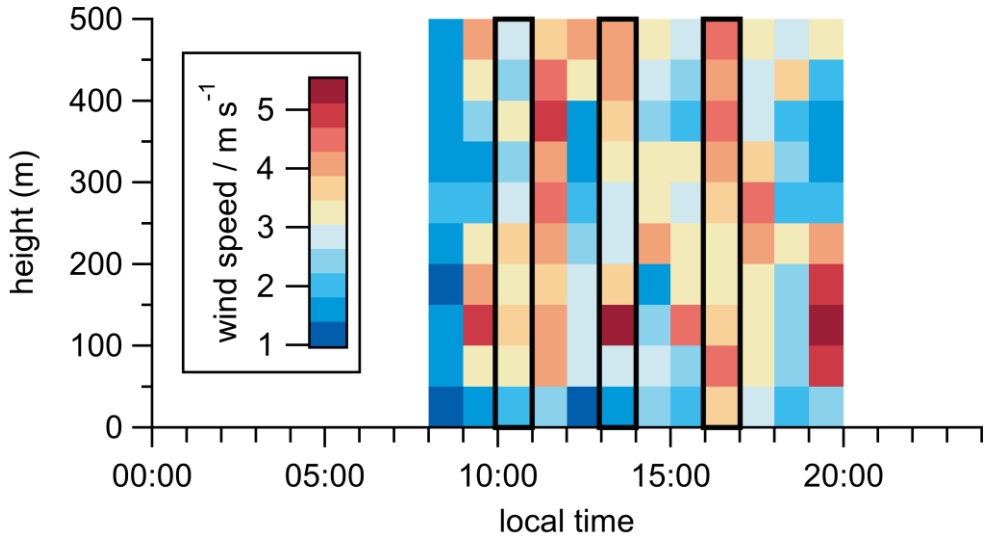

Figure S5: Measured wind speed versus time of day. The measurements were carried out hourly in an altitude range from 0 to 500 m. The black boxes indicate the time intervals during when the parallel UAV flights were conducted.

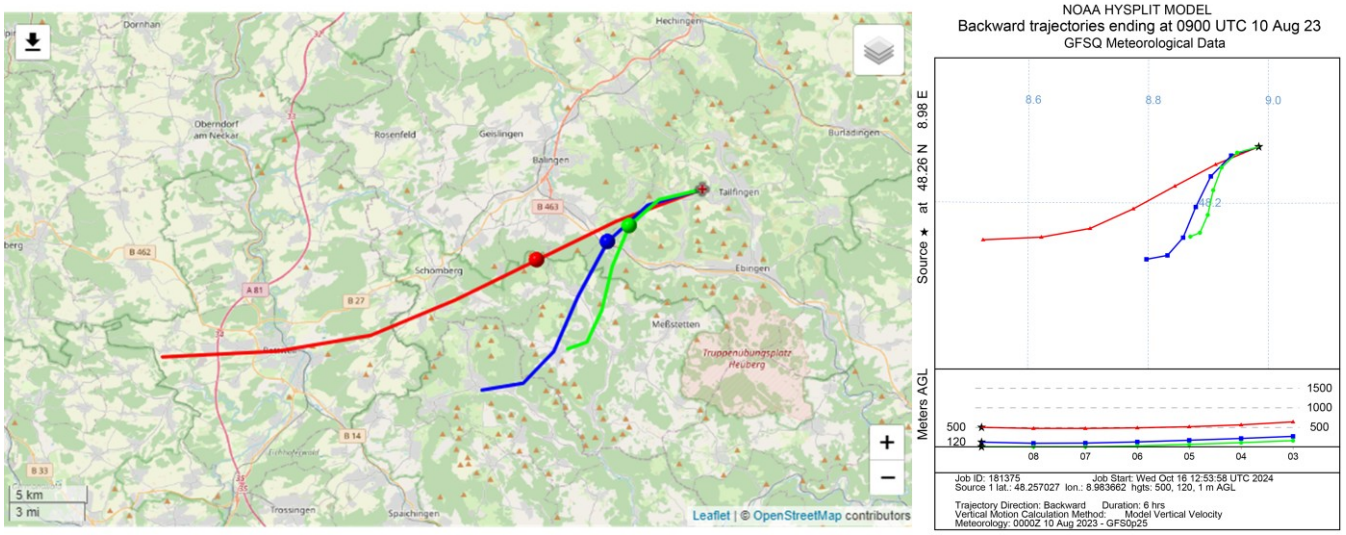

Figure S6: Calculated 6 hour back trajectories with HYSPLIT (Rolph et al., 2017; Stein et al., 2015; Draxler and Hess, 1998) for 1 m (green line), 120 m (blue line) and 500 m (red line) for the sampling on 10.08.2023 in the morning. The dots on the map (© OpenStreetMap contributors 2025. Distributed under the Open Data Commons Open Database License (ODbL) v1.0.) indicate the time (8 am local time) at which the air mass at 120 m altitude crosses the main traffic road.

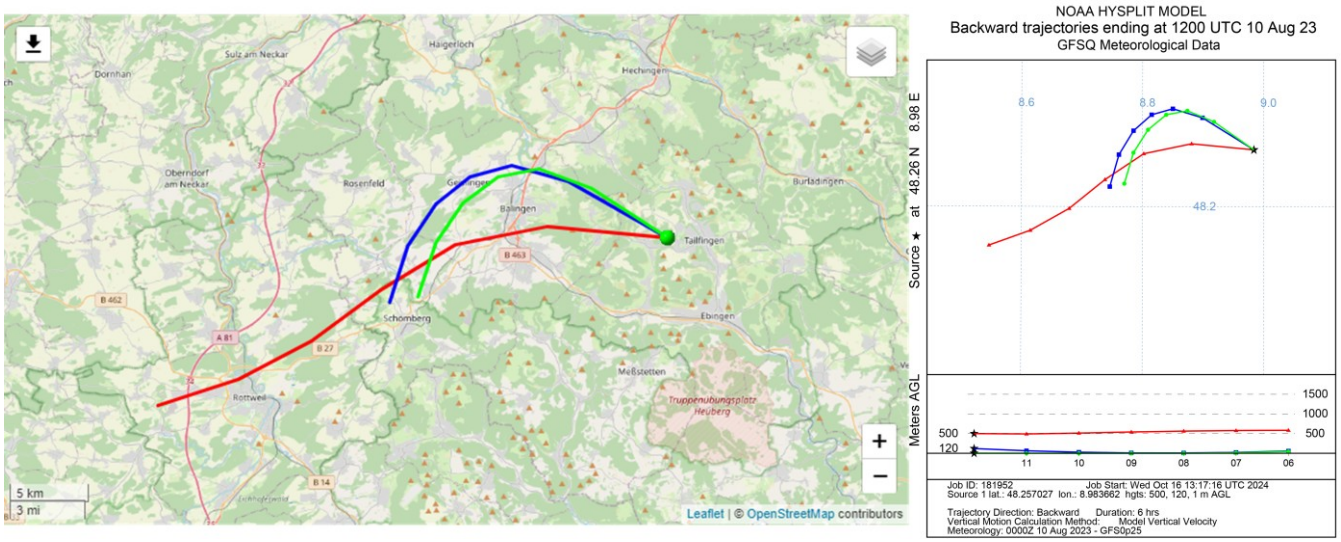

Figure S7: Calculated 6 hour back trajectories with HYSPLIT(Rolph et al., 2017; Stein et al., 2015; Draxler and Hess, 1998) for 1 m (green line), 120 m (blue line) and 500 m (red line) for the sampling on 10.08.2023 at noon (© OpenStreetMap contributors 2025. Distributed under the Open Data Commons Open Database License (ODbL) v1.0.).

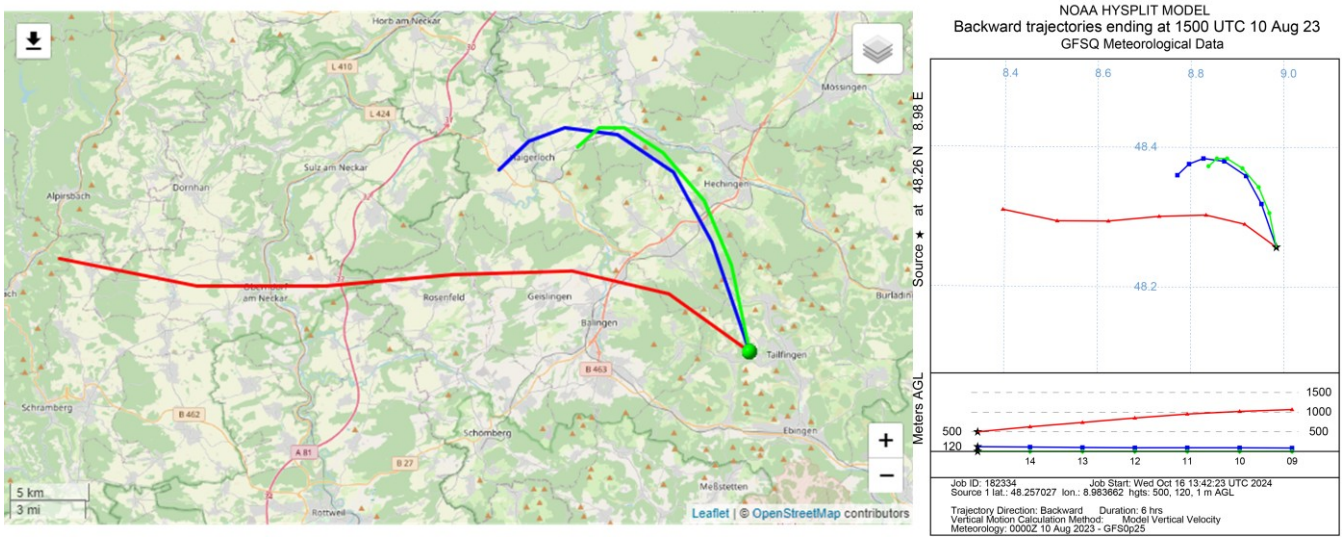

Figure S8: Calculated 6 hour back trajectories with HYSPLIT (Rolph et al., 2017; Stein et al., 2015; Draxler and Hess, 1998) for 1 m (green line), 120 m (blue line) and 500 m (red line) for the sampling on 10.08.2023 in the afternoon (© OpenStreetMap contributors 2025. Distributed under the Open Data Commons Open Database License (ODbL) v1.0.).

References

Draxler, R. R. and Hess, G. D.: An overview of the HYSPLIT_4 modelling system for trajectories, Australian Meteorological Magazine, 47, available at: https://www.researchgate.net/profile/g-hess/publication/239061109_an_overview_of_the_hysplit_4_modelling_system_for_trajectories, 1998.

Rolph, G., Stein, A., and Stunder, B.: Real-time Environmental Applications and Display sYstem: READY, Environmental Modelling & Software, 95, 210–228, https://doi.org/10.1016/j.envsoft.2017.06.025, 2017.

Stein, A. F., Draxler, R. R., Rolph, G. D., Stunder, B. J. B., Cohen, M. D., and Ngan, F.: NOAA's HYSPLIT Atmospheric Transport and Dispersion Modeling System, Bulletin of the American Meteorological Society, 96, 2059–2077, https://doi.org/10.1175/BAMS-D-14-00110.1, 2015.